JOC The Journal of Organic Chemistry

Article

pubs.acs.org/joc

Water-Soluble Bis-triazolyl Benzochalcogendiazole Cycloadducts as Tunable Metal Ion Sensors

Jonathan J. Bryant, Benjamin D. Lindner, and Uwe H. F. Bunz*

Organisch Chemisches Institut, Universität Heidelberg, Im Neuenheimer Feld 270, Heidelberg 69120, Germany

Supporting Information

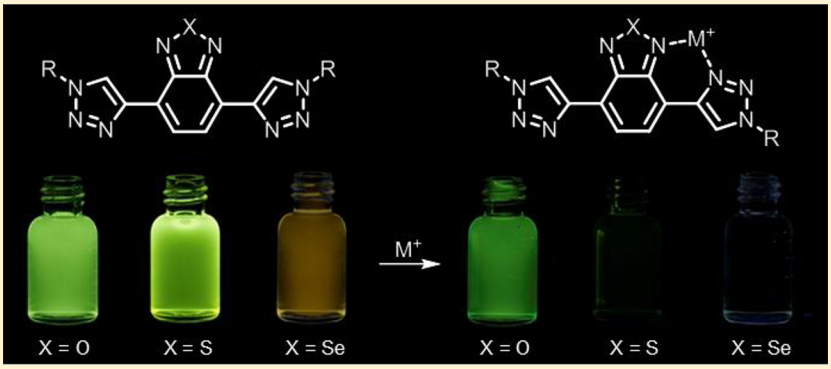

ABSTRACT: A series of bis-triazolyl benzochalcogendiazoles was synthesized to investigate their metal-binding capabilities. These fluorophores were formed through the cycloaddition of an ethynylated benzochalcogendiazole and a water-soluble azide. Variation of the chalcogen heteroatom was seen to affect the photophysical properties as well as the metal-binding activity. These cycloadducts exhibited a distinct response to Cu^{2+}, Ni^{2+}, and Ag^{+} in water. The binding affinity for the copper and nickel ions increased moving the chalcogen atom from O to Se. Statistical analysis of the spectral data enabled differentiation of Ag^{+}, Cu^{2+}, and Ni^{2+} ions.

INTRODUCTION

Rapid and efficient detection of metal ions in aqueous environments is highly sought after. The presence of metal ions in the environment and in biological systems has spurred great interest in their detection and quantification.[1] Traditional methods such as atomic absorption spectroscopy and mass spectrometry are elaborate and time-consuming; fluorescence methods are increasingly being called upon due to their simplicity, sensitivity, and possible in vivo imaging applications.[2−6]

Recent years have seen the development of a large number of fluorescent sensors for metal ions, incorporating small molecules and polymeric systems.[7−17] One shortcoming of many of these fluorescent sensors is their limited solubility in water. This often results in metal ion detection being undertaken in organic solvent or a mixture of organic solvent (such as THF or DMF) with water. For practical purposes, aqueous media is ideal. We have met this challenge by using a branched oligo(ethylene glycol) substituent. This solves the water-solubility issue, and also preserves the fluorescence in water by inhibiting aggregation of the fluorophore.[18,19]

The fluorescent target molecules are synthesized through a copper-catalyzed azide−alkyne cycloaddition. This famous "click" reaction[20,21] has found widespread popularity as a convenient organic linker,[22] including in metal-sensing systems.[23] More recently, the triazole group has been incorporated into fluorescent systems as a functional metal-binding component.[24−27] Here we employ both of these functions, connecting a water-soluble side chain to a heteroaromatic core via a triazole lingake. The end result is a water-soluble fluorophore capable of metal ion recognition in water.

Previous work in our laboratory has involved "tuning" the optical properties of heteroaromatic alkynylated compounds.[28] This has been achieved through the use of substituents and also through variation of the heteroatom. Halogen substitution affects the electronic properties of such heteroaromatic systems and, subsequently, the metal-binding properties of the corresponding bis-triazolyl trimers.[29] In this work, we inquire further as to the "tunability" of the metal-binding activity. Variation of the chalcogen atom in ethynylated benzochalcogendiazoles affects the electronic properties; here, we take a look at the concurrent effect on the metal-binding properties of their corresponding bis-triazolyl cycloadducts.

RESULTS AND DISCUSSION

The synthesis of **3a−c** was achieved through a copper-catalyzed azide−alkyne cycloaddition (Scheme 1). Attempts at a one-pot synthesis from **1b** and **1c** failed to yield any cycloaddition

Received: November 13, 2012
Published: December 27, 2012

dx.doi.org/10.1021/jo3024889 | J. Org. Chem. 2013, 78, 1038−1044

Scheme 1. Synthesis of 3a–c

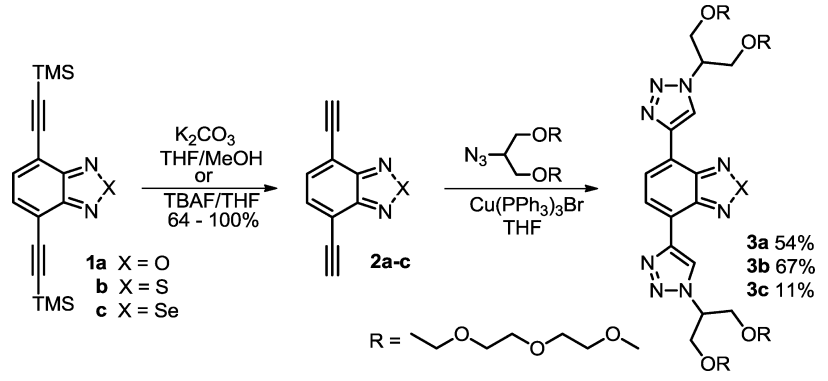

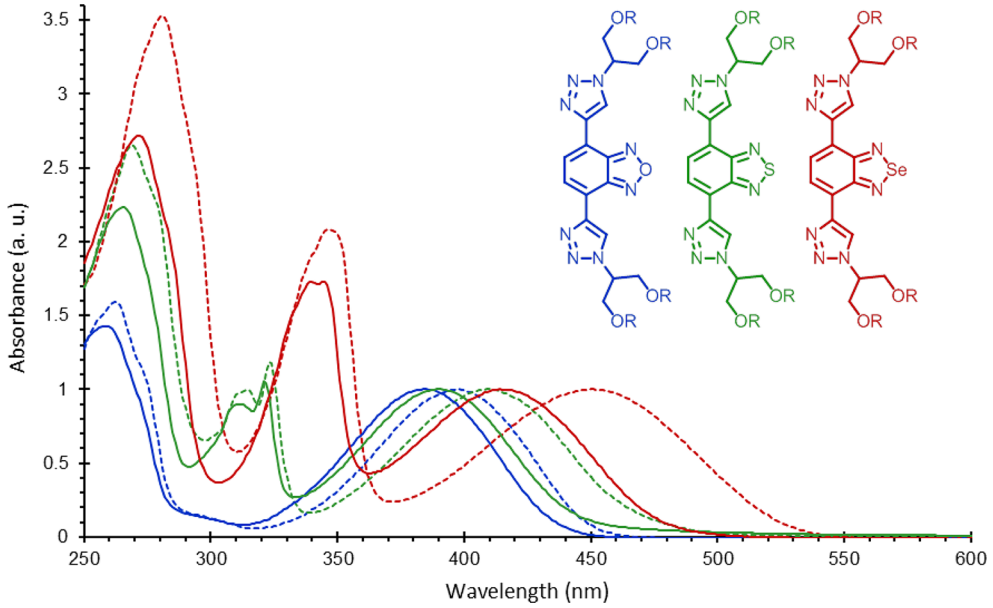

Figure 1. Absorption spectra of **3a–c** in DCM (dashed line) and H_2O (solid line).

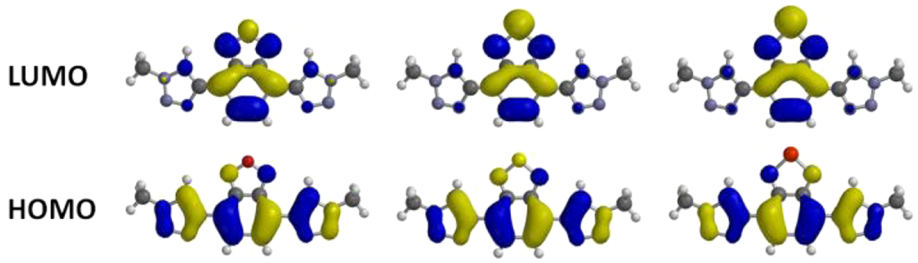

Figure 2. Calculated molecular orbitals for **3a–c** (left to right). Calculated with SPARTAN 10 (B3LYP 6-311++G**// B3LYP 6-311++G**).

product. It was required to first isolate **2a–c**. Removal of the silyl protecting group proceeded rapidly using potassium carbonate for **1a** and **1b**, and tetrabutylammonium fluoride for **1c**. The products **2a–c** degrade rapidly, which made it necessary to use them immediately after purification. Yields for the cycloaddition were moderate, with the exception of **3c**.

Compounds **3a–c** are soluble in both organic and aqueous solvent. The absorption spectra are shown in Figure 1. Shifting the heteroatom down the periodic table from oxygen to selenium serves to red-shift the absorption bands; in particular, the lower energy $S_0 \rightarrow S_1$ transition is shifted significantly more than the higher energy transitions. Also of interest is the decrease in intensity of the lower-energy band relative to the highest energy absorption upon moving to heavier chalcogen atoms, possibly indicating decreasing charge transfer character.

Comparing aqueous and organic solvent, the absorption profiles are hypsochromically shifted in water. Presumably the lowest energy band is due to the $n-\pi^*$ transition, and the hydrogen-bonding interactions of **3a–c** in H_2O serve to stabilize the ground state, resulting in a negative solvatochromism.[30] This effect is not seen with the higher energy absorption bands, which likely represent $\pi-\pi^*$ transitions.

Quantum chemical calculations were performed using SPARTAN molecular modeling software. For simplicity, the ethylene glycol substituent is approximated by a methyl group. Figure 2 shows the calculated frontier orbitals. The HOMOs

dx.doi.org/10.1021/jo3024889 | J. Org. Chem. 2013, 78, 1038–1044

are localized mainly on the triazole axis, and the LUMOs predominantly on the benzochalcogendiazole axis. According to the calculated frontier orbital energies (Table 1), stabilization of the LUMO and destabilization of the HOMO contribute to the observed red-shifts in the photophysical spectra. The change in the LUMO energies from **3a** (−2.96 eV) to **3b** (−2.89 eV) to **3c** (−3.01) indicates that multiple factors influence the energy, and thus the band gap. Treating these cycloadducts as donor−acceptor (D−A) systems, the more electronegative oxygen atom is expected to increase the D−A interaction, thus lowering the band gap. Experimental evidence shows the opposite trend;[31,32] it is thought that the lower ionization potential of the heavier chalcogen atoms, along with the effect on the bond length alternation of the acceptor system (resulting in decreased aromatic character), trumps the D−A interaction, resulting in a lowering of the band gap on switching the chalcogen atom from oxygen to selenium.

Table 1. Calculated and Experimental HOMO−LUMO Gaps

compd	HOMO[a] (eV)	LUMO[a] (eV)	calcd gap (eV)	exptl gap[b] (eV)
3a	−6.18	−2.96	3.22	3.22
3b	−5.98	−2.89	3.09	3.18
3c	−5.91	−3.01	2.90	3.00

[a]Calculated with SPARTAN 10 using the B3LYP method with the 6-311++G** basis set. [b]Acquired from the λ_{max} of absorption in H_2O.

Compounds **3a−c** are yellow in solution, and their fluorescence ranges from blue-green to orange. The fluorescence spectra are shown in Figure 3. The fluorescence is slightly red-shifted in H_2O compared to DCM. The photophysical properties are listed in Table 2; **3a** and **3b** are brightly fluorescent in water, with quantum yields of 0.23 and 0.27, respectively. The lifetimes are shortened in water compared to DCM, though still longer than the average lifetime of cellular autofluorescence (1.9 ns).[33] The large Stokes shifts allow the excitation wavelength to be far removed from the detection wavelength, avoiding interference from the excitation source. These emissive properties suggest these fluorophores as promising candidates for imaging applications. Similar Stokes shifts and lifetimes were observed with bis-triazolyl phenazine fluorophores,[29] highlighting the impact of the triazole on the photophysical properties of these systems.

Table 2. Photophysical Data for 3a−c

compd	abs λ_{max} (nm)	em λ_{max} (nm)	Stokes shift (cm^{-1})	Φ_f (±0.1)	τ_f (ns)
3a (DCM)	397	510	5581	0.64	10
3b (DCM)	410	519	5122	0.66	15
3c (DCM)	450	559	4861	0.40	17
3a (H_2O)	385	525	6926	0.23	6.8
3b (H_2O)	390	528	6702	0.27	11
3c (H_2O)	414	576	6266	0.04	4.1

Next we examined the metal-binding properties of the cycloadducts in water. Screened metal ions include Na^+, K^+, Li^+, Mg^{2+}, Ca^{2+}, Cd^{2+}, Hg^{2+}, Pb^{2+}, Zn^{2+}, Cu^{2+}, Ni^{2+}, and Ag^+; the latter three acted as fluorescence quenchers, although the effect due to Ag^+ was significantly smaller. All three fluorophores exhibited a response to silver ions. Copper and nickel quenched the fluorescence of **3b** and **3c**, but the effect on **3a** was minimal. In order to quantify the binding strength, fluorescence titrations were performed with Ag^+, and also with Cu^{2+} and Ni^{2+} for **3b** and **3c** (Figure 4 and Supporting Information).

We envision the binding conformation to be such that a pocket (Scheme 2) is formed between the N3 of the triazole and the nitrogen of the core molecule. The conformation of this type of trimer is typically that which maximizes the hydrogen bonding available (as shown in Figure 3, inset). Thus, the addition of a metal ion induces a conformational switching into the conformation shown in the graphical abstract and Scheme 2, previously noted by our group and others.[29,34] To determine the binding stoichiometry, the method of continuous variation, or Job's plot, was used (see the Supporting Information). The largest change is seen at a 1:1 stoichiometry. When the titration data were fitted to the standard Stern−Volmer equation, only the Cu^{2+} and Ni^{2+} data resulted in an

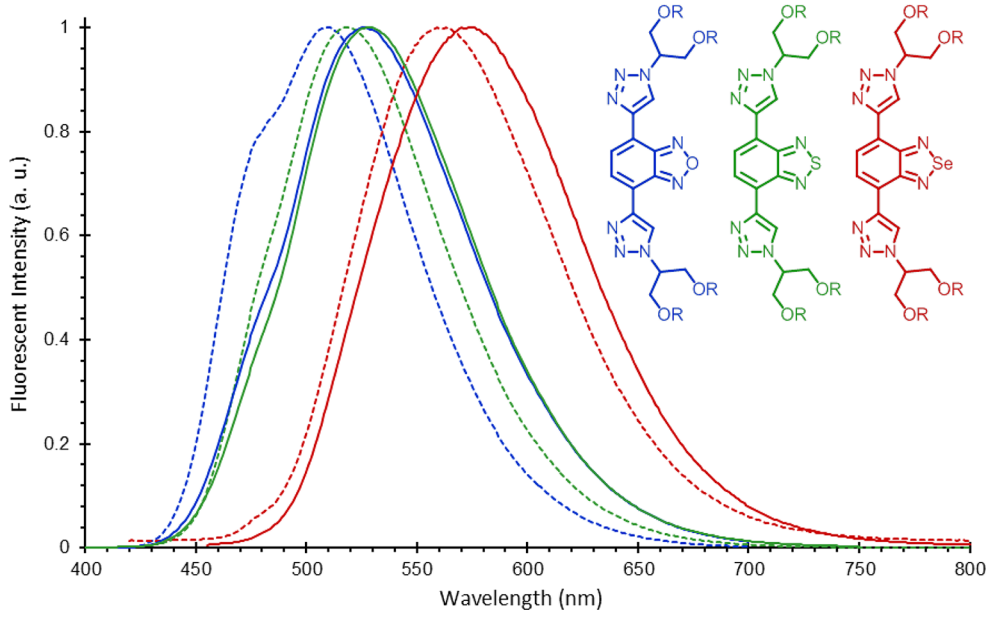

Figure 3. Fluorescence spectra of **3a−c** in DCM (dashed line) and H_2O (solid line).

dx.doi.org/10.1021/jo3024889 | J. Org. Chem. 2013, 78, 1038−1044

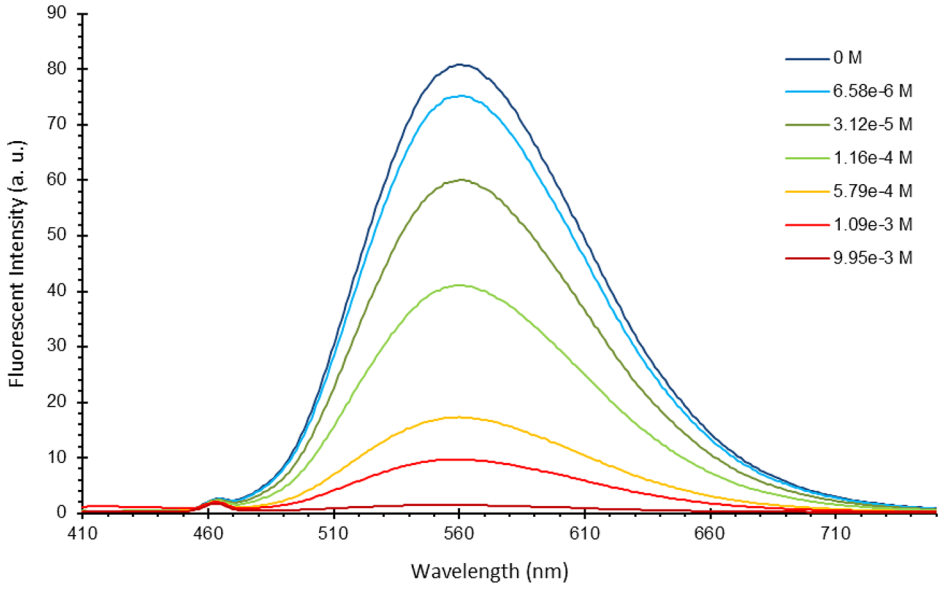

Figure 4. Fluorescence titration of **3b** with Ni^{2+}.

Scheme 2. Schematic Binding Mode of 3b to Nickel Salts

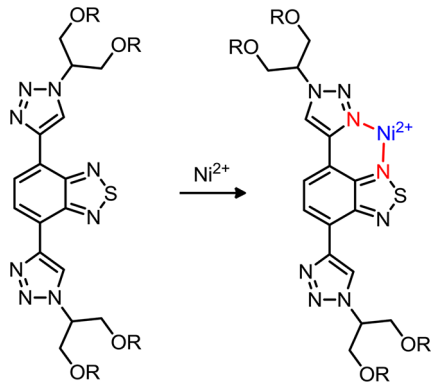

acceptable fit. However, all the data were able to be fitted using eq 1.[35−37]

$$\Delta I = \frac{\alpha}{2}\left\{\left([F] + [Q] + \frac{1}{K}\right) - \sqrt{\left([F] + [Q] + \frac{1}{K}\right)^2 - 4[F][Q]}\right\} \quad (1)$$

ΔI is the change in fluorescent intensity, $[F]$ is the concentration of the fluorophore, and $[Q]$ is the concentration of the quencher. The variable α is a proportionality constant relating the fluorescence intensity to the concentration of the fluorophore. This equation is derived directly from the equilibrium expression for the formation of the 1:1 metal/fluorophore complex, where the binding constant K is the association constant. The equilibrium expression involves the concentrations of the free fluorophore and quencher, which may be substituted as seen in eq 2.

$$K = \frac{[FQ]}{([F] - [FQ])([Q] - [FQ])} \quad (2)$$

Equation 2 contains the concentration of the complex, which is unknown. If the initial fluorescence is proportional to the initial concentration of fluorophore ($I_0 = \alpha_1[F]$) and the fluorescence at any given time is the sum of the fluorescent contributions from the fluorophore and complex ($I = \alpha_1[F]_{free} + \alpha_2[FQ]$), then the change in the fluorescence is proportional to the concentration of the complex ($\Delta I = \alpha[FQ]$). Equation 1 is reached by substituting for $[FQ]$ in eq 2 and solving for ΔI. K can then be determined through a least-squares curve fitting. Seeing that application of eq 1 for the Cu^{2+} and Ni^{2+} data resulted in binding constants very similar to what was determined from the Stern−Volmer analysis, this equation was used to determine the binding constant for all the data.

The binding constants are shown in Table 3. The values determined for **3b** are comparable to those found previously for

Table 3. Binding Constants (Reported as log[K])

compd	Cu^{2+}	Ni^{2+}	Ag^{+}
3a			3.80 ± 0.11
3b	2.40 ± 0.07	2.60 ± 0.04	3.73 ± 0.12
3c	4.25 ± 0.09	4.13 ± 0.07	4.08 ± 0.14

a similar bis-triazolyl compound with triethylene glycol substituents.[38] Binding of copper and nickel ions is heavily influenced by the chalcogen heteroatom, with **3c** being the most sensitive. This may be due to a number of factors, including aromaticity and size, but the decreasing electronegativity of the chalcogen atom (going from O to Se) is the most likely suspect. The binding to silver is unaffected by the chalcogen atom, resulting in similar binding constants for all three fluorophores. Unexpectedly, binding of Ag^{+} results in only minimal fluorescence quenching. Unlike the Stern−Volmer equation, formation of a nonfluorescent complex is not an assumption inherent in eq 1, and the binding constants are still able to be extracted from the fluorescence data.

A response from three different metals begs the question of whether some selectivity can be imparted. Examination of the UV−vis spectra from the metal titrations reveals unique responses to each metal. Linear discriminant analysis (LDA)[39] was used to analyze the differences in the absorption spectra, whereby each metal can be identified according to the characteristic response of the fluorophore. Absorbance titration

dx.doi.org/10.1021/jo3024889 | J. Org. Chem. 2013, 78, 1038−1044

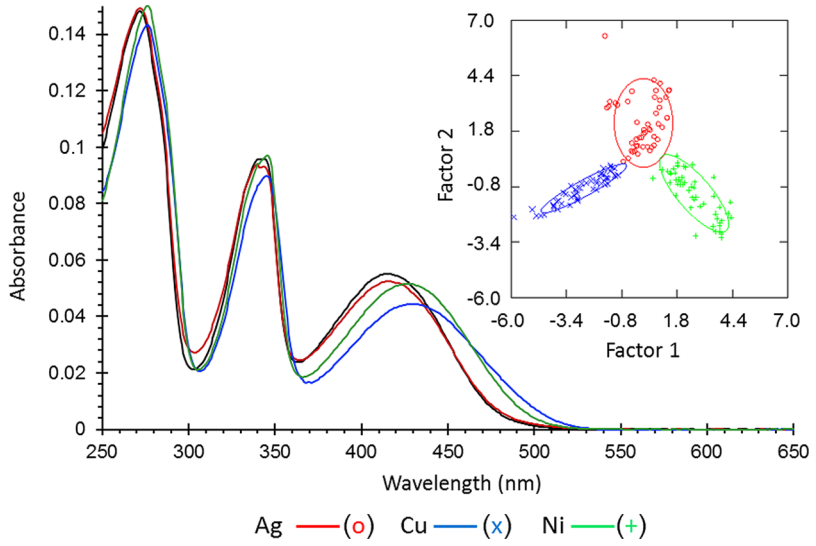

Figure 5. Absorption spectra of **3c** in H_2O without metal ion (black trace) and with different metal ions at 116 μM concentrations. Inset: The corresponding canonical scores plot generated from the linear discriminant analysis.

data with Ag^+, Cu^{2+}, and Ni^{2+} were collected at a constant concentration of **3c**, with the metal ion concentration ranging from 6 to 600 μM (see the Supporting Information). The collected spectral data were preprocessed by subtracting the initial absorption spectrum, where the concentration of metal is zero, so that the analysis was performed using the change in the absorbance. LDA is then able to classify each spectrum as belonging to one of the three metals, based on the unique spectral changes (Figure 5).

Each data point in the canonical scores plot represents an absorbance spectrum at a certain concentration of metal. To confirm the accuracy of this method, each individual spectrum can be treated as an unknown, and then classified as one of the three metals. Using this cross-validation technique, we found 100% classification accuracy for metal ion concentrations above 15 μM, though the limits of detection of **3c** for the individual metals Ag^+, Cu^{2+}, and Ni^{2+} were determined to be 3.8, 0.27, and 0.56 μM, respectively. Copper and nickel ions can be accurately discriminated from each other at concentrations below 7 μM. Addition of silver ion to the analysis clouds the picture somewhat, and metal concentrations below 15 μM result in inaccuracies. The range of concentrations used in the titrations indicates that this identification technique is not dependent on concentration, and because the analysis is performed using the change in absorbance, it is largely independent of the fluorophore concentration as well. It should be noted that quantification of the metal ion concentration is a straightforward matter when the binding constant is known.

CONCLUSION

In summary, we have synthesized a series of water-soluble, highly fluorescent metal sensors with tunable properties. These compounds utilize a triazole ring to form a binding pocket for metal ions. Our investigation of the chalcogen-property relationship in these compounds reveals a lowering of the band gap on going from oxygen to selenium, as well as an increase in the binding efficiency of copper and nickel ions. Statistical analysis of the spectrophotometric response of **3c** to the different metal ions results in a sensitive and selective sensor for silver, copper, and nickel, ideal for use in aqueous systems. More research, however, is needed to obtain lower detection limits, useful for the control of industrial effluvia and wastewater streams containing these metal ions.

EXPERIMENTAL SECTION

Quantum yield measurements were determined relative to quinine sulfate in dilute sulfuric acid. Time-correlated single photon counting lifetime measurements were made with a pulsed laser diode.

4,7-Bis(trimethylsilyl)ethynylbenzo[*c*][1,2,5]oxadiazole (1a). 4,7-Dibromobenzo[*c*][1,2,5]oxadiazole[28] (94 mg, 0.34 mmol), $Pd(PPh_3)_2Cl_2$ (2.4 mg, 0.0034 mmol), and CuI (1.3 mg, 0.0068 μmol) were dissolved in THF (4 mL) and triethylamine (1 mL) in a Schlenk tube. The solution was then deoxygenated by freezing and evacuating (3×). After the solution was warmed to room temperature and the Schlenk tube was sealed under nitrogen gas, trimethylsilylacetylene (0.13 g, 1.4 mmol) was added via syringe. The reaction was stirred at room temperature for 18 h. The solids were then filtered, and the solution was extracted with saturated aqueous NH_4Cl (25 mL) and DCM (2 × 25 mL). The organic fractions were collected and dried over magnesium sulfate, the solvent was evaporated, and the product was purified by silica gel chromatography (100:1 hexanes/EtOAc) to yield **1a** as a yellow solid (64 mg, 0.20 mmol, 60%). Mp: 86−88 °C. IR (cm^{-1}): 2957, 2898, 2156, 1592, 1550, 1530, 1378, 1250, 1065, 1004, 838, 761, 699. ^1H NMR (300 MHz, $CDCl_3$): δ = 7.46 (s, 2H), 0.30 (s, 18 H). ^{13}C NMR (75 MHz, $CDCl_3$): δ = 149.4, 135.0, 112.9, 106.0, 98.3, −0.2. HRMS (EI) *m*/*z*: $[M]^+$ calcd for $C_{16}H_{20}N_2OSi_2$ = 312.1114, found =312.1130.

4,7-Bis(trimethylsilyl)ethynylbenzo[*c*][1,2,5]thiadiazole (1b). 4,7-Dibromobenzo[*c*][1,2,5]thiadiazole[40] (2.0 g, 6.8 mmol), $Pd(PPh_3)_2Cl_2$ (0.19 g, 0.27 mmol), and CuI (0.10 g, 0.27 mmol) were dissolved in THF (40 mL) and triethylamine (10 mL) in a Schlenk tube. The solution was then deoxygenated by freezing and evacuating (3×). After the solution was warmed to room temperature and the Schlenk tube sealed under nitrogen gas, trimethylsilylacetylene (2.0 g, 0.020 mol) was added via syringe. The reaction was stirred at room temperature for 48 h. The solids were then filtered, the solvent was evaporated, and the product was purified by silica gel chromatography (200:1 hexanes/EtOAc) to yield **1b** as a light tan solid (1.8 g, 5.5 mmol, 81%). Mp: 114−115 °C. IR (cm^{-1}): 2955, 2898, 2153, 1560, 1539, 1491, 1338, 1245, 1031, 836, 758, 640. ^1H NMR (300 MHz, $CDCl_3$): δ = 7.70 (s, 2H), 0.33 (s, 18H). ^{13}C NMR (75 MHz, $CDCl_3$): δ = 154.4, 133.3, 117.4, 103.8, 100.2, 0.03. HRMS (EI) *m*/*z*: $[M]^+$ calcd for $C_{16}H_{20}N_2SSi_2$ = 328.0886, found = 328.0898.

4,7-Bis(trimethylsilyl)ethynylbenzo[*c*][1,2,5]selenodiazole (1c). A solution of selenium dioxide (0.185 g, 1.66 mmol) in hot H_2O (1 mL) was added to a solution of 3,6-bis((trimethylsilyl)ethynyl)-

dx.doi.org/10.1021/jo3024889 | J. Org. Chem. 2013, 78, 1038−1044

benzene-1,2-diamine[29] (0.100 g, 0.333 mmol) in EtOH (15 mL) at 60 °C. The reaction was stirred until full conversion was reached according to TLC. The reaction mixture was then filtered, and the precipitate was washed with water. Purification by silica gel chromatography (hexanes → 50:1 hexanes/EtOAc) gave **1c** as a yellow crystalline solid (0.113 g, 0.301 mmol, 90%). Mp: 172−175 °C. IR (cm^{-1}): 2960, 2898, 2148, 1560, 1520, 1474, 1354, 1245, 1037, 1014, 833, 758, 633. ^1H NMR (300 MHz, $CDCl_3$): δ = 7.60 (s, 2H), 0.31 (s, 18H). ^{13}C NMR (75 MHz, $CDCl_3$): δ = 159.2, 133.6, 119.1, 103.5, 100.7, 0.06. HRMS (EI) m/z: $[M]^+$ calcd for $C_{16}H_{20}N_2SeSi_2$ = 376.0330, found = 376.0334. Correct isotope distribution: Anal. Calcd for $C_{16}H_{20}N_2SeSi_2$: C, 51.18; H, 5.37; N, 7.46. Found: C, 50.97; H, 5.52; N, 7.56.

4,7-Diethynylbenzo[*c*][1,2,5]oxadiazole (2a). Compound **1a** (64 mg, 0.20 mmol) and K_2CO_3 (0.28 g, 2.0 mmol) were stirred into 1:1 MeOH/THF (10 mL) for 15 min. The solids were then filtered, the solvent was evaporated, and the residue was purified by silica gel chromatography (50:1 hexanes/EtOAc) to give **2a** as a faint yellow, light-sensitive solid (33 mg, 0.20 mmol, 100%). Mp: 82 °C dec. IR (cm^{-1}): 3313, 3269, 2923, 2853, 2106, 1767, 1552, 993, 866, 618. ^1H NMR (300 MHz, $CDCl_3$): δ = 7.55 (s, 2H), 3.70 (s, 2H). ^{13}C NMR (75 MHz, $CDCl_3$): δ = 149.7, 135.6, 112.8, 87.4, 77.6. HRMS (EI) m/z: $[M]^+$ calcd for $C_{10}H_4N_2O$ 168.0324, found 168.0327.

4,7-Diethynylbenzo[*c*][1,2,5]thiadiazole (2b). Compound **1a** (1.61 g, 4.78 mmol) was dissolved in a 1:1 THF/MeOH solution (50 mL). K_2CO_3 (3.3 g, 24 mmol) was added as a solution in H_2O (10 mL), and the reaction mixture was stirred overnight (16 h). The solution was extracted with H_2O (40 mL) and DCM (3 × 50 mL). Purification by silica gel chromatography (50:1 hexanes/EtOAc) gave an orange, light-sensitive solid (0.560 g, 3.04 mmol, 64%). Mp: 114 °C (decomposition). IR (cm^{-1}): 3276, 3053, 2108, 1892, 1541, 1489, 1478, 881, 848, 670, 611. ^1H NMR (300 MHz, $CDCl_3$): δ = 7.75 (s, 2H), 3.67 (s, 2H). ^{13}C NMR (75 MHz, $CDCl_3$): δ = 154.5, 133.4, 116.9, 85.5, 79.0. MS (EI) m/z: $[M]^+$ calcd for $C_{10}H_4N_2S$ = 184.0, found = 184.0.

4,7-Diethynylbenzo[*c*][1,2,5]selenadiazole (2c). Compound **1c** (0.100 g, 0.266 mmol) was dissolved in THF (10 mL). A 1.0 M solution of tetrabutylammonium fluoride in THF (1.7 mL, 1.7 mmol) was added very slowly, and the reaction was stirred for 5 min. The solvent was then removed under reduced pressure, and purification by silica gel chromatography (1:1 $CHCl_3$/hexanes) afforded **2c** as a yellow-orange solid (0.0480 g, 0.208 mmol, 78%). Mp: 109 °C dec. IR (cm^{-1}): 3266, 3045, 2129, 2100, 1885, 1698, 1523, 1483, 847, 610. ^1H NMR (300 MHz, $CDCl_3$): δ = 7.67 (s, 2H), 3.67 (s, 2H). ^{13}C NMR (75 MHz, $CDCl_3$): δ = 159.2, 133.6, 118.7, 85.3, 79.5. HRMS (EI) m/z: $[M]^+$ calcd for $C_{10}H_4N_2Se$ = 231.9540, found = 231.9540.

4,7-Bis(1-(2,5,8,11,15,18,21,24-octaoxapentacosan-13-yl)-1*H*-1,2,3-triazol-4-yl)benzo[*c*][1,2,5]oxadiazole (3a). Compound **2a** (0.017 g, 0.10 mmol) and 13-azido-2,5,8,11,15,18,21,24-octaoxapentacosane[29] (0.10 g, 0.25 mmol) were dissolved in THF (2 mL). The mixture was degassed via the freeze/pump/thaw method (3×), and $Cu(PPh_3)_3Br$ (0.0090 g, 0.010 mmol) was added under a flow of nitrogen. The solution was then stirred at room temperature overnight (16 h), during which time a green fluorescence developed. The solution was extracted with saturated aqueous NH_4Cl (30 mL) and DCM (3 × 50 mL). Purification by silica gel chromatography (9:1 EtOAc/MeOH) yielded an orange oil (0.054 g, 0.055 mmol, 54%). IR (cm^{-1}): 2918, 2870, 1450, 1349, 1236, 1097, 937, 873. ^1H NMR (300 MHz, $CDCl_3$): δ = 8.65 (s, 2H), 8.40 (s, 2H), 5.05 (quin, J = 6.0 Hz, 2H), 4.02 (m, 4H), 3.66−3.56 (m, 41H), 3.50 (m, 8H), 3.33 (s, 12H). ^{13}C NMR (75 MHz, $CDCl_3$): δ = 147.6, 141.5, 127.2, 124.4, 118.6, 72.01, 71.10, 70.74, 70.71, 70.59, 70.14, 61.3, 59.1. HRMS (ESI) m/z: $[M + H]^+$ calcd for $C_{44}H_{75}N_8O_{17}$ = 986.5250, found = 987.5246.

4,7-Bis(1-(2,5,8,11,15,18,21,24-octaoxapentacosan-13-yl)-1*H*-1,2,3-triazol-4-yl)benzo[*c*][1,2,5]thiadiazole (3b). Compound **2b** (0.090 g, 0.49 mmol) and 13-azido-2,5,8,11,15,18,21,24-octaoxapentacosane[29] (0.50 g, 1.2 mmol) were dissolved in THF (10 mL). The mixture was degassed via the freeze/pump/thaw method (3×), and $Cu(PPh_3)_3Br$ (0.045 g, 0.049 mmol) was added under a flow of nitrogen. The solution was then stirred at 50 °C overnight (16 h), during which time a green color and intense green fluorescence developed. The solution was extracted with H_2O (70 mL) and DCM (5 × 20 mL) until the aqueous phase was no longer fluorescent. The organic portions were collected and washed with saturated aqueous NH_4Cl (25 mL). Purification by silica gel chromatography (5:1 EtOAc/MeOH) yielded **3b** as an orange oil (0.33 g, 0.33 mmol, 68%). IR (cm^{-1}): 2870, 1704, 1447, 1352, 1236, 1095, 878, 847. ^1H NMR (300 MHz, $CDCl_3$): δ = 8.87 (s, 2H), 8.61 (s, 2H), 5.03 (m, 2H), 4.01 (d, J = 6.0 Hz, 8H), 3.65−3.51 (m, 41H), 3.46 (m, 8H), 3.29 (s, 12H). ^{13}C NMR (75 MHz, $CDCl_3$): δ = 152.3, 142.7, 125.9, 124.3, 122.8, 71.86, 70.96, 70.58, 70.56, 70.45, 70.14, 61.0, 59.0. HRMS (ESI) m/z: $[M + H]^+$ calcd for $C_{44}H_{75}N_8O_{16}S$ = 1003.5022, found = 1003.5030.

4,7-Bis(1-(2,5,8,11,15,18,21,24-octaoxapentacosan-13-yl)-1*H*-1,2,3-triazol-4-yl)benzo[*c*][1,2,5]selenadiazole (3c). Compound **2c** (0.048 g, 0.21 mmol) and 13-azido-2,5,8,11,15,18,21,24-octaoxapentacosane[29] (0.21 g, 0.52 mmol) were dissolved in THF (10 mL). The mixture was degassed via the freeze/pump/thaw method (3×) and $Cu(PPh_3)_3Br$ (0.020 g, 0.021 mmol) was added under a flow of nitrogen. The solution was then stirred at 50 °C overnight (16 h). The solution turned black and intensely green fluorescent after only 3 h. The solution was extracted with H_2O (30 mL) and DCM (5 × 50 mL) until the aqueous phase was no longer fluorescent. The organic portions were collected and washed with saturated aqueous NH_4Cl (25 mL). Purification by silica gel chromatography (9:1 EtOAc:-MeOH) yielded **3c** as an orange oil (0.023 g, 0.022 mmol, 11%). IR (cm^{-1}): 2870, 2097, 1723, 1637, 1453, 1352, 1250, 1200, 1097, 934, 849, 542. ^1H NMR (300 MHz, $CDCl_3$): δ = 8.87 (s, 2H), 8.56 (s, 2H), 5.03 (quin, J = 6.0 Hz, 2H), 4.03 (d, J = 6.0 Hz, 7H), 3.65−3.55 (m, 48H), 3.49 (m, 8H), 3.33 (s, 13H). ^{13}C NMR (75 MHz, $CDCl_3$): δ = 158.0, 143.1, 126.4, 124.9, 124.3, 72.00, 71.09, 70.72, 70.69, 70.59, 70.57, 70.29, 61.1, 59.1. HRMS (ESI) m/z: $[M + H]^+$ calcd for $C_{44}H_{75}N_8O_{16}Se$ = 1051.4466, found = 1051.4489.

■ ASSOCIATED CONTENT

Supporting Information

NMR spectra, tables of Cartesian coordinates, and additional plots and spectra. This material is available free of charge via the Internet at http://pubs.acs.org.

■ AUTHOR INFORMATION

Corresponding Author

*E-mail: uwe.bunz@oci.uni-heidelberg.de.

Notes

The authors declare no competing financial interest.

■ REFERENCES

(1) Quang, D. T.; Kim, J. S. *Chem. Rev.* **2010**, *10*, 6280.
(2) Qian, X.; Xiao, Y.; Xu, Y.; Guo, X.; Qian, J.; Zhu, W. *Chem. Commun.* **2010**, *46*, 6418.
(3) Tan, S. S.; Teo, Y. N.; Kool, E. T. *Org. Lett.* **2010**, *12*, 4820.
(4) Winkler, J. D.; Bowen, C. M.; Michelet, V. *J. Am. Chem. Soc.* **1998**, *120*, 3237.
(5) Jeong, Y.; Yoon, J. *Inorg. Chim. Acta* **2012**, *381*, 2.
(6) Zhang, J. F.; Zhou, Y.; Yoon, J.; Kim, J. S. *Chem. Soc. Rev.* **2011**, *134*, 3416.
(7) Formica, M.; Fusi, V.; Giorgi, L.; Micheloni, M. *Coord. Chem. Rev.* **2012**, *256*, 170.
(8) Zhang, J. F.; Zhou, Y.; Yoon, J.; Kim, J. S. *Chem. Soc. Rev.* **2011**, *40*, 3416.
(9) Kim, H. N.; Ren, W. X.; Kim, J. S.; Yoon, J. *Chem Soc. Rev.* **2012**, *41*, 3210.
(10) Sun, H.-B.; Liu, S.-J.; Ma, T.-C.; Song, N.-N.; Zhao, Q.; Huang, W. *New J. Chem.* **2011**, *35*, 1194.
(11) Bao, Y.; Wang, H.; Li, Q.; Liu, B.; Li, Q.; Bai, W.; Jin, B.; Bai, R. *Macromolecules* **2012**, *45*, 3394.
(12) Li, C.; Zhou, C.; Zheng, H.; Yin, X.; Zuo, Z.; Liu, H.; Li, Y. *J. Polym. Sci., Part A: Polym. Chem.* **2008**, *46*, 1998.

(13) Kim, I.-B.; Erdogan, B.; Wilson, J. N.; Bunz, U. H. F. *Chem.—Eur. J.* **2004**, *10*, 6247.
(14) Zucchero, A. J.; Wilson, J. N.; Bunz, U. H. F. *J. Am. Chem. Soc.* **2006**, *128*, 11872.
(15) Zucchero, A. J.; McGrier, P. L.; Bunz, U. H. F. *Acc. Chem. Res.* **2010**, *43*, 397.
(16) Tolosa, J.; Zucchero, A. J.; Bunz, U. H. F. *J. Am. Chem. Soc.* **2008**, *130*, 6498.
(17) Wilson, J. N.; Bunz, U. H. F. *J. Am. Chem. Soc.* **2005**, *127*, 4124.
(18) Khan, A.; Müller, S.; Hecht, S. *Chem. Commun.* **2005**, 584.
(19) Kim, I.-B.; Phillips, R.; Bunz, U. H. F. *Macromolecules* **2007**, *40*, 5290.
(20) Tornoe, C. W.; Christensen, C.; Meldal, M. *J. Org. Chem.* **2002**, *67*, 3057.
(21) Rostovtsev, V. V.; Green, L. G.; Fokin, V. V.; Sharpless, K. B. *Angew. Chem., Int. Ed.* **2002**, *41*, 2596.
(22) Theme Issue 4, Applications of Click Chemistry: *Chem. Soc. Rev.* **2010**, *39*, 1221.
(23) Pathak, R. K.; Dikundwar, A. G.; Row, T. N. G.; Rao, C. P. *Chem. Commun.* **2010**, *46*, 4345.
(24) Schweinfurth, D.; Hardcastle, K. I.; Bunz, U. H. F. *Chem. Commun.* **2008**, *19*, 2203.
(25) Lau, H. Y.; Rutledge, P. J.; Watkinson, M.; Todd, M. H. *Chem. Soc. Rev.* **2011**, *40*, 2848.
(26) Vedamalai, M.; Wu, S.-P. *Eur. J. Org. Chem.* **2012**, *2012*, 1158.
(27) Neupane, L. N.; Kim, J. M.; Lohani, C. R.; Lee, K.-H. *J. Mater. Chem.* **2012**, *22*, 4003.
(28) Coombs, B. A.; Lindner, B. D.; Edkins, R. M.; Rominger, F.; Beeby, A.; Bunz, U. H. F. *New J. Chem.* **2012**, *36*, 550.
(29) Bryant, J. J.; Zhang, Y.; Lindner, B. D.; Davey, E. A.; Appleton, A. L.; Qian, X.; Bunz, U. H. F. *J. Org. Chem.* **2012**, *77*, 7479.
(30) Reichardt, C. *Solvents and Solvent Effects in Organic Chemistry*: Wiley-VCH: Weinheim, 2003.
(31) Das, S.; Pati, P. B.; Zade, S. S. *Macromolecules* **2012**, *45*, 5410.
(32) Gibson, G. L.; McCormick, T. M.; Seferos, D. S. *J. Am. Chem. Soc.* **2012**, *134*, 539.
(33) Knemeyer, J.-P.; Herten, D.-P.; Sauer, M. *Anal. Chem.* **2003**, *75*, 2147.
(34) Meudtner, R. M.; Ostermeier, M.; Goddard, R.; Limberg, C.; Hecht, S. *Chem.—Eur. J.* **2007**, *13*, 9834.
(35) Liu, Y.; Chen, Y.; Li, L.; Zhang, H.-Y.; Liu, S.-X.; Guan, X.-D. *J. Org. Chem.* **2001**, *66*, 8518.
(36) You, C. C.; De, M.; Han, G.; Rotello, V. M. *J. Am. Chem. Soc.* **2005**, *127*, 12873.
(37) Phillips, R. L.; Miranda, O. R.; Mortenson, D. E.; Subramani, C.; Rotello, V. M.; Bunz, U. H. F. *Soft Matter* **2009**, *5*, 607.
(38) Brombosz, S. M.; Appleton, A. L.; Zappas, A. J.; Bunz, U. H. F. *Chem. Commun.* **2010**, *46*, 1419.
(39) Performed using commercially available software SYSTAT13.
(40) Bangcuyo, C. G.; Evans, U.; Myrick, M. L.; Bunz, U. H. F. *Macromolecules* **2001**, *34*, 7592.